

Buckling of stainless steel columns in fire

S. Afshan

Brunel University London, London, UK

O. Zhao, L. Gardner, E. Ho

Imperial College London, London, UK

ABSTRACT:

The inherent corrosion resistance and elevated temperature strength retention of stainless steels lend themselves to applications in buildings and structures where fire resistance is important. This paper examines the fire resistance design of stainless steel columns, and in particular focuses on the suitability of using the 0.2% proof stress $f_{0.2}$ or the stress at 2% total strain f_2 as the basic design strength parameters. Through analysis of FE generated column data, it is shown that the 0.2% proof stress is a more appropriate parameter as the basis for derivation of the buckling curves for stainless steel columns.

1 INTRODUCTION

The corrosion resistance and durability of stainless steel are well known, offering the potential for more sustainable construction with increased structural design lives. Stainless steel is most commonly used in structures in the offshore and onshore industrial sector (e.g. oil and gas, petrochemical, pharmaceutical, nuclear, etc.) where fire is a significant hazard. Other applications that utilize the fire resistance of stainless steel are in light interior structures (e.g. escape routes in airports and office buildings), and in safety critical structures (e.g. locations exposed to terrorist attack). Hence, development of comprehensive and economic guidance for the design of stainless steel structures in fire is of paramount importance if the use of the material in fire safety critical applications is to increase. A number of recent studies have indicated that the fire resistance of stainless steel structural members is greater than that of equivalent carbon steel members (Gardner, 2007 and Gardner and Baddoo, 2006). With superior strength and stiffness retention at elevated temperatures, in comparison with carbon steels, stainless steels potentially offer substantial improvements in performance.

The fire resistant design of structural carbon steels is covered in EN 1993-1-2 (2005). EN 1993-1-4 (2006) which is the part of Eurocode 3 that provides supplementary design rules for stainless steel structures refers to EN 1993-1-2 (2005) for their fire design, where the same guidelines as those for carbon steels are also adopted for stainless steels. How-

ever, the stress-strain behaviour of stainless steels is of different form to that of carbon steels. Whereas carbon steels typically exhibit linear elastic behaviour up to the yield strength and a plateau before strain hardening, stainless steels possess a more rounded response with no well-defined yield strength. This results in a difference in the structural behaviour between carbon steels and stainless steels, and consequently different design rules will be needed in certain cases. A fundamental example of this is related to the design strength parameter f_y used to determine the fire resistance of structural components. EN 1993-1-2 (2005) employs the strength at 2% total strain f_2 i.e. $f_y = f_2$ for Classes 1, 2 and 3 cross-sections, and the 0.2% proof stress $f_{0.2}$ i.e. $f_y = f_{0.2}$ for Class 4 cross-sections in determining the resistance, for all types of loading, of structural steel members in fire. The use of the 2% strength is to reflect the allowance for greater deformations in fire, which enables higher member strengths to be developed. These strength parameters are also adopted for the fire design of stainless steel structures in EN 1993-1-4 (2006). However, the design of structural components at member level, e.g. columns and unrestrained beams, is mainly controlled by material stiffness, which reduces significantly beyond the yield point, which is in the region of the 0.2% proof stress point for stainless steels. This means that the design buckling curves, e.g. the χ factors in Eurocode 3 for column design, should be derived based on the strength level that triggers member buckling, i.e. $f_{0.2}$ rather than f_2 . Hence, the suitability of these two strength parameters, f_2 and $f_{0.2}$, to de-

termine the fire resistance of stainless steel compression members is investigated in this paper. A comprehensive numerical modeling study has been conducted to generate the structural performance data necessary for this investigation. The development of the finite element models, including their validation against existing test results, as well as the results of the parametric studies, which were performed subsequently, are presented.

2 NUMERICAL MODELLING

Numerical models for predicting the resistance of stainless steel columns in fire were developed using the non-linear finite element analysis package ABAQUS (2015). The models were first validated against experimental results and subsequently used to perform parametric studies. The development of the numerical models and the results of the parametric studies are described hereafter.

2.1 Validation of numerical models

2.1.1 Overview

The results of fire tests on square hollow section (SHS) and rectangular hollow section (RHS) columns including three grade EN 1.4003 columns reported by Rossi (2012), six grade EN 1.4301 columns reported by Ala Outinen and Oksanen (1997) and three grade EN 1.4301 columns reported by Gardner and Baddoo (2006) were used for the validation of the finite element models. A summary of these tests is provided in Tables 1 and 2. All fire tests were performed anisothermally, whereby the load was applied at room temperature and was maintained at a constant level while the temperature was increased until failure at θ_{crit} . For each model, a sequentially coupled thermal-stress analysis was carried out, involving three types of numerical analyses - (1) a heat transfer analysis to obtain the temperature development in the structural members, (2) a linear elastic buckling analysis to determine the buckling mode shapes and finally (3) a geometrically and materially non-linear stress analysis, which incorporated the temperature field from (1) and the buckling mode shapes as imperfections from (2).

Table 1: Summary of ferritic tests Rossi (2012).

Nominal section size	Boundary condition	Load (kN)	$\theta_{crit, furnace}$ (°C)
SHS 80×80×3-3000	Fixed	72	709
SHS 80×80×3-2500	Fixed	78	708
RHS 120×80×3-2500	Fixed	100	705

2.1.2 Heat transfer model

The measured specimen time-temperature data was used in modelling the austenitic stainless steel

Table 2: Summary of austenitic tests Gardner and Baddoo (2006).

Nominal section size	Boundary condition	Load (kN)	$\theta_{crit, specimen}$ (°C)
RHS 150×100×6	Fixed	268	801
RHS 150×75×6	Fixed	140	883
RHS 100×75×6	Fixed	156	806

Table 3: Summary of austenitic tests from Ala Outinen and Oksanen (1997).

Nominal section size	Boundary condition	Load (kN)	$\theta_{crit, specimen}$ (°C)
SHS 40×40×4 (T1)	Pinned	45	872
SHS 40×40×4 (T2)	Pinned	129	579
SHS 40×40×4 (T3)	Pinned	114	649
SHS 40×40×4 (T4)	Pinned	95	710
SHS 40×40×4 (T5)	Pinned	55	832
SHS 40×40×4 (T7)	Pinned	75	766

columns. For the ferritic column tests, the specimen temperature was not measured during the tests; only the furnace temperature was measured. Hence, heat transfer analyses were first carried out to obtain the evolution of specimen temperature with the fire exposure time for the ferritic columns, which was required as input for the stress analysis part of the modelling procedure. The thermal analysis of a structural member can be divided into two parts: the heat transfer from the fire to the exposed surface of the structural element through combined convection and radiation heat transfer mechanisms, and conductive heat transfer within the structural member itself; these were accurately simulated in the FE models.

2.1.3 Stress analysis model

The non-linear stress analysis was performed in two steps to simulate the anisothermal loading condition of the column tests. In the first step, the load was applied to the column at room temperature. This load was maintained at a constant level during the second step while the evolution of the temperature with the fire exposure time, from the heat transfer analysis, was applied. For the case of the austenitic stainless steel columns, the mean measured steel surface temperature was directly imported into the models.

2.1.4 General modelling assumptions

Shell elements were adopted to simulate the stainless steel tubular hollow section columns, as is customary for the modelling of thin-walled structures. The four-node doubly curved general-purpose shell element with reduced integration S4R, for the structural model, and D4S, for the thermal model, which has performed well in numerous similar applications (Ashraf et al., 2006; Ng and Gardner, 2007; To and Young, 2008) was used. A suitable mesh size, providing accurate results with practical computational times, with a minimum of ten elements across each plate was adopted. The test boundary condi-

tions were replicated by restraining suitable displacement and rotation degrees of freedom at the column ends. Measured geometric dimensions were used in each model to replicate the corresponding test specimen.

2.1.5 Material and thermal properties

The accuracy of finite element models is highly dependent on the prescribed material parameters, hence making a precise representation of the material characteristics essential. For the ferritic stainless steel column tests, the modified compound Ramberg-Osgood material model for elevated temperatures proposed by Gardner et al. (2010), along with the measured elevated temperature reduction factors for the EN 1.4003 grade from Afshan (2013) and the measured room temperature material properties were used. For the case of the austenitic column tests, the measured flat material stress-strain curves at elevated temperatures were directly utilized in the development of the finite element models. The strength enhancements in the corner regions of the SHS and RHS specimens were also incorporated in the FE models. ABAQUS requires that the material properties are specified in terms of true stress σ_{true} and log plastic strain ϵ_{ln}^p , which may be derived from the nominal engineering stress-strain curves as defined in Equations (1) and (2), respectively, where σ_{nom} and ϵ_{nom} are engineering stress and strain, respectively and E is the Young's modulus.

$$\sigma_{\text{true}} = \sigma_{\text{nom}}(1 + \epsilon_{\text{nom}}) \quad (1)$$

$$\epsilon_{\text{ln}}^p = \ln(1 + \epsilon_{\text{nom}}) - \frac{\sigma_{\text{true}}}{E} \quad (2)$$

For the austenitic stainless steel columns, the thermal properties from EN 1993-1-2 (2005) were used in the models. The thermal properties of ferritic stainless steels are different from austenitic stainless steels and are not currently covered in EN 1993-1-2 (2005). For the EN 1.4003 grade, thermal expansion data were sourced from EN 10088-1 (2005) and specific heat and thermal conductivity data were obtained from the StahlDat SX (2011) database.

2.1.6 Geometric imperfections and residual stresses

The lowest local and global buckling mode shapes, determined by means of an elastic eigenvalue buckling analysis, were assumed for the respective imperfection patterns along the member length and incorporated into the FE models. Global imperfection amplitude of $L/2000$, where L is the column total length, was adopted for the austenitic stainless steel columns, in the absence of measured values, while the measured imperfection amplitudes of the test specimens were used for the ferritic stainless steel columns. For the local imperfection amplitude w_0 , values predicted by the Dawson and Walker model, as adapted for stainless steel (Ashraf et al., 2006)

given by Equation (3), were used, where t is the plate thickness, $f_{0.2}$ is the material 0.2% proof stress and σ_{cr} is the plate elastic buckling stress. Through thickness bending residual stresses were not explicitly included in the FE models since their effect is inherently present in the measured material properties used, which were obtained from coupons cut from the finished tubes (Ashraf et al., 2006). The effect of membrane residual stresses was considered negligible, and was therefore not included in the FE models.

$$w_0 = 0.023t(f_{0.2}/\sigma_{\text{cr}}) \quad (3)$$

2.1.7 Validation results

A total of 9 austenitic and 3 ferritic stainless steel columns were modelled using the sequentially coupled thermal-stress analysis procedure described. The fire performance criteria set out in EN 1363-1 (1999) for vertically loaded members were used to determine the critical failure temperature of the columns. It states that a column is deemed to have failed when both the vertical contraction and the rate of vertical contraction have exceeded $L/100$ mm and $3L/1000$ mm/min, respectively, where L is initial column height in mm. Figure 1 compares the test axial deformation versus temperature results with the FE results for the SHS $80 \times 80 \times 3$ -2500 ferritic column. A summary of the comparisons between the test and FE results is provided in Table 4. For the austenitic stainless steel columns, the FE models give a mean FE/test critical temperature of 0.90 and a coefficient of variation of 0.03, and provide safe-side predictions of the fire resistance of the test column specimens. For the ferritic stainless steel columns, the FE and test results are in very good agreement with a mean FE/test critical temperature of 1.00 and a coefficient of variation of 0.02. From the comparison of the test and FE results, it is concluded that the described FE models are capable of safely replicating the non-linear, large deflection response of the stainless steel columns in fire.

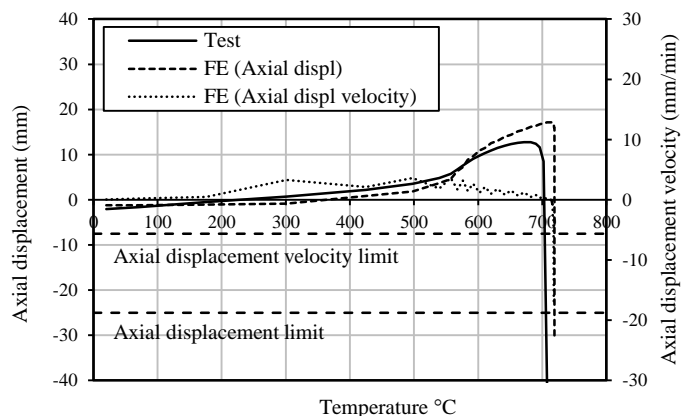


Figure 1: Vertical displacement versus temperature of SHS $80 \times 80 \times 3$ -2500 specimen.

Table 4: Comparison of critical temperatures between test and FE results.

Nominal section size	Critical temperature (°C)		
	Test	FE	Test/FE
SHS 80×80×3-3000	709	726	1.02
SHS 80×80×3-2500	708	718	1.02
RHS 120×80×3-2500	705	709	1.01
RHS 150×100×6	801	757	0.91
RHS 150×75×6	883	814	0.92
RHS 100×75×6	806	744	0.92
SHS 40×40×4 (T1)	872	750	0.86
SHS 40×40×4 (T2)	579	502	0.87
SHS 40×40×4 (T3)	649	608	0.94
SHS 40×40×4 (T4)	710	646	0.91
SHS 40×40×4 (T5)	832	722	0.87
SHS 40×40×4 (T7)	766	681	0.89

2.2 Parametric studies

Having validated the FE models, a series of parametric studies was performed to generate further structural performance data over a range of member slenderness values, allowing an assessment of the EN 1993-1-2 and EN 1993-1-4 buckling curves for the design of stainless steel compression members in fire. Since the stress-strain response and the elevated temperature material properties of stainless steels vary between the different grades, parametric studies were performed for the two most common austenitic and duplex stainless steels. Also, since the focus was on the flexural buckling response of stainless steel compression members, a limited number of fixed cross-section geometries with varying member lengths were modelled for each of the stainless steel grades. For modelling convenience, all parametric study models were performed isothermally, where the material properties for a given temperature θ were incorporated into the FE models, akin to applying a uniform temperature θ , and the applied load was increased until failure. A static Riks analysis procedure was used to trace the load-deformation response of each of the modelled columns and to determine their failure load. This approach was deemed acceptable, since the influence of time dependent effects, e.g. creep, was not included in the developed FE models, and therefore both the isothermal and anisothermal modelling approaches would yield very similar results.

The outer dimensions of the austenitic and duplex SHS parametric study models were fixed to 100×100 and 150×150, respectively. Two different thicknesses were then selected for each of the considered grades such that one Class 1 and one Class 3 cross-sections were modelled in each case. Columns of varying lengths, modelled as pin-ended at both ends, provided a range of room temperature member slenderness $\bar{\lambda}$ from 0.1 to 3.0. The room temperature material properties for the flat faces and the corner regions pertaining to the cold-formed SHS 100×100×5

(Austenitic 1.4301) and SHS 150×150×8 (Duplex 1.4162) measured in Afshan et al. (2013) were employed. Strength and stiffness reduction factors, defined as the ratio of the strength or stiffness at elevated temperature θ to their values at room temperature are generally used to define material properties at elevated temperature; these are $k_{E,\theta}$, $k_{0.2,\theta}$, $k_{u,\theta}$ for the stiffness E , the 0.2% proof stress $f_{0.2}$ and the ultimate tensile strength f_u . The strength at 2% total strain $f_{2\%}$ is defined in EN 1993-1-2 (2005) using a different approach, as described by Equation (4), and values for the $k_{2,\theta}$ are provided in the code.

$$f_2 = f_{0.2} + k_{2,\theta}(f_u - f_{0.2}) \quad (4)$$

The stiffness reduction factors $k_{E,\theta}$ provided in EN 1993-1-2 were adopted for both studied stainless steel grades. A series of strength reduction factors $k_{0.2,\theta}$, $k_{u,\theta}$ and $k_{2,\theta}$ rationalised on the basis of grouping stainless steel grades that exhibit similar elevated temperature properties were proposed by Gardner et al. (2010). The reduction factors belonging to the stainless steel groups containing the studied austenitic 1.4301 and duplex 1.4162 grades were therefore adopted. The modified Ramberg-Osgood material model proposed in Ashraf et al. (2006), along with the adopted elevated temperature reduction factors, and the room temperature material properties were used to develop full-range stress-strain curves at discrete temperatures of 20 °C-900 °C. The Ramberg-Osgood model parameters n and n' at room temperature were also adopted in developing the full range stress-strain curves at elevated temperature. The same modelling assumptions as explained in the previous sections were employed. The global imperfection amplitude was taken as $L/1000$, where L is the column length, in accordance with the permitted out-of-straightness tolerance in EN 1090-2 (2008). The local imperfection amplitude was taken as that predicted by Equation (3). All columns were pin-ended at both ends. Owing to the symmetry in the geometry and the boundary conditions of the models, only half of the section, and half of the member length, was modelled.

3 ANALYSIS OF RESULTS AND RECOMMENDATIONS

The fire design of stainless steel structures is covered in EN 1993-1-2 (2005) with similar treatments to carbon steel structures. Provisions more specific to stainless steel structures are also provided in the Euro-Inox/SCI Design Manual for Stainless Steel (2006), and in the literature (Ng and Gardner, 2007; Uppfeldt et al., 2008 and Lopez et. al., 2010). In determining the buckling resistance of stainless steel columns in fire, in EN 1993-1-2, similar to carbon

steels, the elevated temperature stress at 2% total strain f_2 is used for Class 1, 2 and 3 cross-sections, while the elevated temperature 0.2% proof stress $f_{0.2}$ is employed for Class 4 cross-sections. However, the use of the stress at 2% total strain f_2 for predicting the buckling resistance of members, which is mainly controlled by material stiffness, which reduces significantly beyond the 0.2% proof stress point, is considered to be inappropriate for stainless steels.

Since the difference between the strength at 2% total strain f_2 and the 0.2% proof stress $f_{0.2}$ are relatively small for carbon steels, the column buckling curves, i.e. the χ factors in Eurocode 3, derived based on either strength parameter, f_2 and $f_{0.2}$, are essentially the same. However, this is not the case for stainless steels, which typically show a considerable amount of strain hardening, resulting in f_2 values which are substantially higher than the $f_{0.2}$ values. Hence, different buckling curves are obtained depending on which strength parameter, f_2 or $f_{0.2}$, is used to normalize the column failure loads. In addition, the $f_2/f_{0.2}$ ratio varies between the different stainless steel grades and also with temperature. It is higher for the austenitic and duplex grades, than the ferritic grades, as these show greater levels of strain hardening. This means that different buckling curves will be obtained for different stainless steel grades, and also for different temperatures, if the column buckling curves are established in terms of the elevated temperature f_2 rather than the elevated temperature $f_{0.2}$, which is approximately the stress reached in the most heavily stressed cross-section of the column at failure. Figure 2 show the variation of the $f_2/f_{0.2}$ ratio with temperature for both studied austenitic and duplex stainless steel grades.

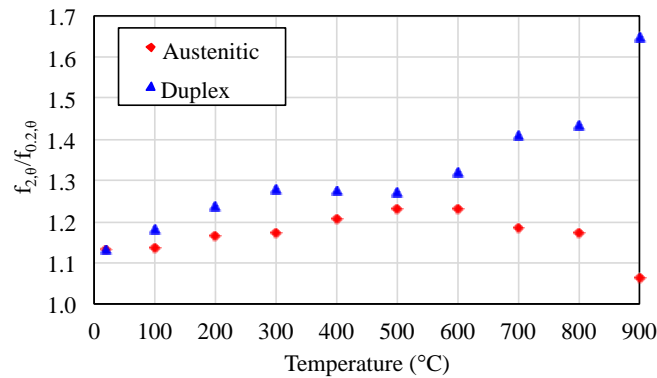


Figure 2: Variation of $f_2/f_{0.2}$ ratio with temperature.

The above mentioned effects are shown in Figures 3-10, where the FE ultimate loads for the austenitic and duplex stainless steel columns have been normalized by the squash loads based on the f_2 or $f_{0.2}$ strength parameters, and are more prominent for the duplex grade, which have higher and more variable $f_2/f_{0.2}$ ratios. As shown in Figures 3 and 5 for the austenitic columns and Figures 7 and 9 for the duplex columns, normalizing the column failure load by the $Af_{0.2}$ squash load, allows all buckling curves

to approximately converge for all temperatures, and avoids the use of temperature dependent buckling curves as proposed in Lopez et al. (2010) based on f_2 . Note that for very stocky columns, buckling effects are minimal and failure loads beyond the $Af_{0.2}$ squash load can be achieved.

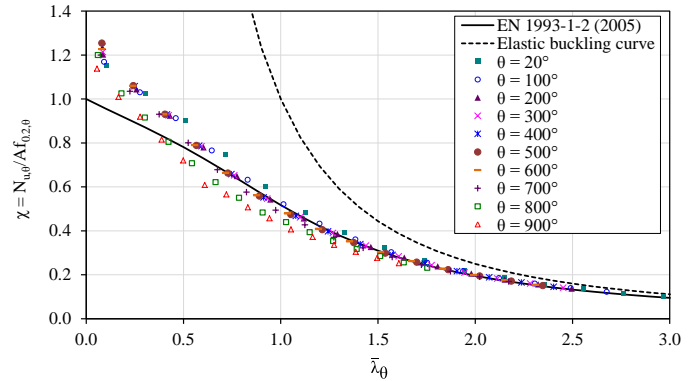


Figure 3: Austenitic Class 1 FE results normalized by $Af_{0.2}$.

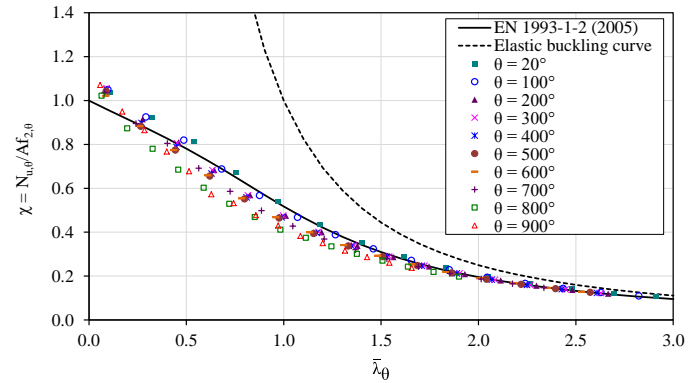


Figure 4: Austenitic Class 1 FE results normalized by Af_2 .

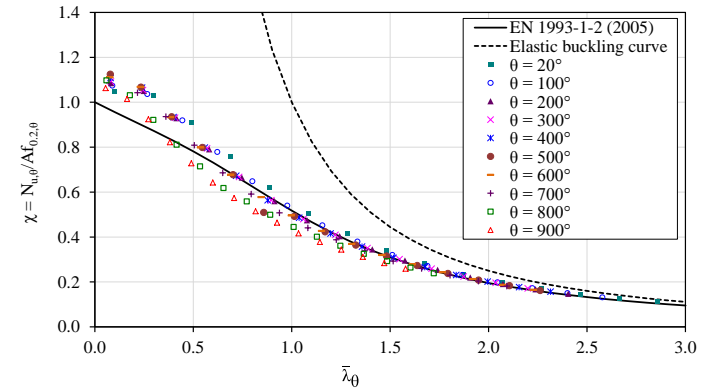


Figure 5: Austenitic Class 3 FE results normalized by $Af_{0.2}$.

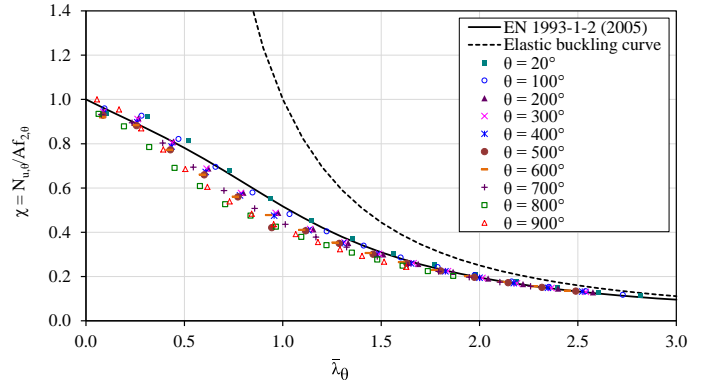


Figure 6: Austenitic Class 3 FE results normalized by Af_2 .

4 CONCLUSIONS

The suitability of using the 0.2% proof stress instead of the stress at 2% total strain for developing buckling curves for the design of stainless steel columns in fire was investigated. Based on the results of the numerical modelling study conducted, it was shown that the 0.2% proof stress, which is the region where there is a sharp reduction in the material stiffness, is in fact more appropriate, and allows grade and temperature independent buckling curves to be established.

5 REFERENCES

- ABAQUS. 2015. ABAQUS, Version 6.12-2. Dassault Systmes Simulia Corp. USA.
- Afshan, S. 2013. Structural behavior of cold-formed stainless steel tubular members. Ph.D. Thesis, Imperial College London, UK.
- Afshan, S., Rossi, B., and Gardner, L. 2013. Strength enhancements in cold-formed structural sections - Part I: Material testing. *Journal of Constructional Steel Research*, 83(0), 177 – 88.
- Ala-Outinen, T., and Oksanen, T. 1997. Stainless steel compression members exposed to fire. Tech. rept. 1864. VTT Building Technology, Helsinki, Finland.
- Ashraf, M., Gardner, L., and Nethercot, D. A. 2006. Finite element modelling of structural stainless steel cross-sections. *Thin-Walled Structures*, 44(10), 1048 – 1062.
- EN 1993-1-2. 2005. Eurocode 3: Design of steel structures - Part 1-2: General rules - Structural fire design. Brussels: European Committee for Standardization.
- EN 1993-1-4. 2006. Eurocode 3: Design of steel structures - Part 1-4: General rules - Supplementary rules for stainless steels. Brussels: European Committee for Standardization.
- EN 1363-1. 1999. Fire resistance tests - Part 1: General requirements. Brussels: European Committee for Standardization.
- EN 10088-1. 2005. Stainless steels - Part 1: List of stainless steels. Brussels: European Committee for Standardization.
- EN 1090-2. 2008. Execution of steel structures and aluminium structures - Part 2: Technical requirements for steel structures. Brussels: European Committee for Standardization.
- Euro-Inox/SCI. 2006. Design manual for structural stainless steel. Third edn. Euro-Inox/SCI.
- Gardner, L. 2007. Stainless steel structures in fire. *Proceedings of the ICE - Structures and Buildings*, 160(SB3), 129 – 138.
- Gardner, L., Insausti, A., Ng, K. T., and Ashraf, M. 2010. Elevated temperature material properties of stainless steel alloys. *Journal of Constructional Steel Research*, 66(5), 634 – 647.
- Gardner, L., and Baddoo, N. R. 2006. Fire testing and design of stainless steel structures. *Journal of Constructional Steel Research*, 62(6), 532 – 543.
- Lopes, N., Vila Real, P., Silva, L. S., and Franssen, J. M. 2010. Axially loaded stainless steel columns in case of fire. *Journal of Structural Fire Engineering*, 1(1), 43 – 59.
- Ng, K. T., and Gardner, L. 2007. Buckling of stainless steel columns and beams in fire. *Engineering Structures*, 29(5), 717 – 730.
- Rossi, B. 2012. Stainless steel in structures in view of sustainability. In: *Fourth international stainless steel experts seminar*. Ascot, UK. SX, Stahldat. 2011. Available at: <http://www.stahldaten.de>. [Accessed: 12 November 2012].
- To, E. C., and Young, B. 2008. Performance of cold-formed stainless steel tubular columns at elevated temperatures. *Engineering Structures*, 30(7), 2012 – 2021.
- Uppfeldt, B., Ala Outinen, T., and Veljkovic, M. 2008. A design model for stainless steel box columns in fire. *Journal of Constructional Steel Research*, 64(11), 1294 – 1301.

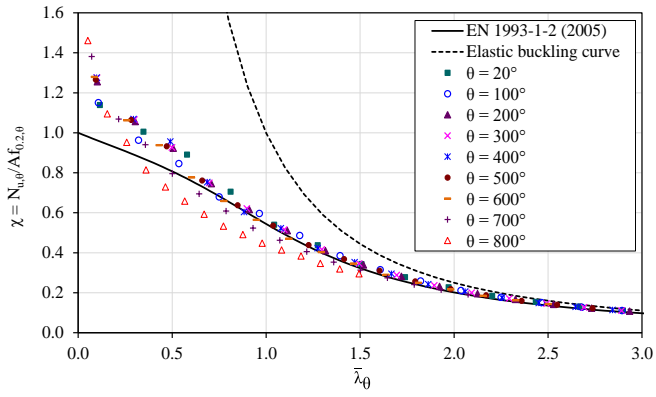


Figure 7: Duplex Class 1 FE results normalized by $Af_{0.2}$.

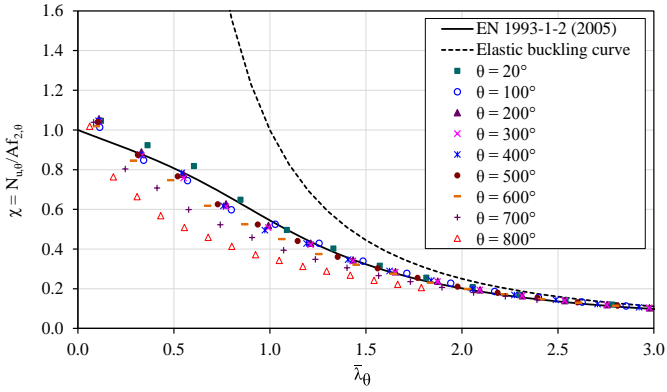


Figure 8: Duplex Class 1 FE results normalized by Af_2 .

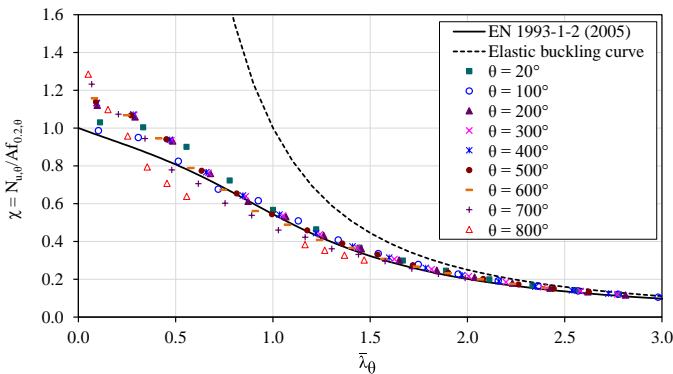


Figure 9: Duplex Class 3 FE results normalized by $Af_{0.2}$.

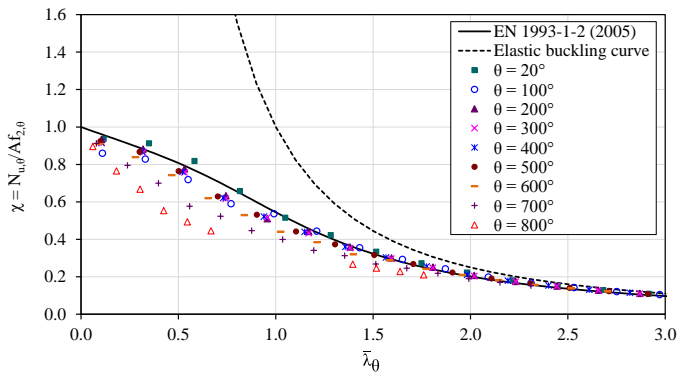


Figure 10: Duplex Class 3 FE results normalized by Af_2 .

Overall, the results presented herein support the use of the 0.2% proof stress rather than the stress at 2% total strain as the basis for developing buckling curves for stainless steel members in fire.